



Investigation of CO Methanation with Different Carbon-Supported Ni-, Fe-, and Co-Containing Catalysts

Filiz Derekaya¹ · Atike Büşra Köprülü¹ · Yusuf Serkan Kiliñç²

Received: 24 February 2022 / Accepted: 29 December 2022 / Published online: 5 January 2023
© King Fahd University of Petroleum & Minerals 2023

Abstract

Catalysts (metaloxide/carbon support) for carbon monoxide methanation were prepared with two different preparation methods using three different metals and three different carbon supports. While nickel (Ni), iron (Fe), and cobalt (Co) were used as metals, graphene oxide, activated carbon and mesoporous carbon were used as carbon support. Two traditional preparation methods, impregnation and co-precipitation, were used in order to prepare the catalysts. The X-ray diffraction, N₂ physisorption, high-resolution transmission electron microscopy, and scanning electron microscopy analysis were used to characterize the catalysts. The CO methanation studies were conducted on all catalysts. The highest surface area results were obtained over the iron oxide composed catalysts. It was found that the impregnation method is the most suitable method for obtaining a high surface area. The average pore diameters of the catalysts entered to the mesopore diameter scale in the Dubinin classification. Except for active carbon-supported iron and cobalt catalysts, other catalysts have crystal phases due to the NiO, Fe₂O₃, and Co₃O₄, according to the composition of catalysts. Activated carbon-supported iron and cobalt catalysts showed an amorphous phase structure. The catalysts prepared by the impregnation method had higher activity. Higher activities were obtained from the graphene oxide supported catalysts. When activities were evaluated in terms of active component (metal oxide) type, cobalt oxide active component provided better results. Co₃O₄/graphene oxide catalyst prepared by the impregnation method leads to 100% CO conversion and 85% CH₄ formation at 275 °C.

Keywords Methane · Carbon monoxide · Hydrogenation · Carbon support · Preparation method

1 Introduction

Carbon is formed in almost all heterogeneous catalytic reactions involving organic molecules. These species are referred to as soot, coke or carbon residues. They are known for their defined graphitic structure and are often harmful forms. These species block the active sites responsible for the reaction activity in the catalyst structure and cause catalyst

deactivation [1]. Carbon is a good catalyst support. This is due to its different pore structure, resistance to acidic and basic environments, low price, easy accessibility, good recycling properties, low density, being synthesized in other ways, or being used in a wide range of engineering, production, activation, and carbonization methods. Solid carbons of different structures are known as polyforms and are composed entirely of carbon in different physical structures. Amorphous carbons and crystalline carbons show two different physical structures [2]. Graphite and diamond are the most well-known forms of crystalline carbon and have a wide range of industrial applications. Fullerene and carbon nanofibers began to be developed in the 1960s and 1970s. The official discovery of carbon nanotubes was made in 1991 by Iijima. These types of carbon materials have wide applications as semiconductor, aerospace, catalysts and gas storage. In addition, some of these materials are used in industrial applications. They perform well in applications such as fuel cells and catalysts. The oldest form of carbon is amorphous carbon. They do not have regular structures and consist

✉ Filiz Derekaya
filizb@gazi.edu.tr

Atike Büşra Köprülü
busrakoprulu123@gmail.com

Yusuf Serkan Kiliñç
yusufserkankinc@gmail.com

¹ Chemical Engineering Department, Faculty of Engineering, Gazi University, 06570 Maltepe, Ankara, Turkey

² Advanced Technologies Department, Graduate School of Natural and Applied Sciences, Gazi University, Teknikokullar, Ankara, Turkey



of strong covalent bonds in the basic structure. Its production and use date back to the nineteenth century. There are also extensive studies on activated carbon. The usefulness of activated carbon stems from its micropore and mesopore volumes, and accordingly, its high surface area feature. According to the studies in recent years, templated carbons have been found as “amorphous” carbon with controllable porosity and structures. Templated carbons are synthesized by using hard and soft preparation techniques with a high surface area ($4100 \text{ m}^2/\text{g}$) and large pore volume ($2.25 \text{ cm}^3/\text{g}$). These properties encourage the use of templated carbons as good catalyst support and adsorbent [2, 3]. Commercial carbons are used as catalyst support material because their porous structure allows the catalyst active component to be dispersed evenly within the pores. Activated carbons, carbon nanotubes, nanofibers, and fullerenes are the most mentioned and widely used catalyst support materials in the literature. In order to improve the catalytic properties and stability of the carbon species, the active metal component of the catalyst is mostly dispersed into the structure by impregnation or precipitation techniques. Porous carbons are used in many applications as adsorbent in separation processes, as a support in catalytic processes, and as electrode material in electrochemical systems. In general, glassy carbon (or vitreous carbons) and graphitic carbons are used in electrodes because of their electron-conducting properties. Carbon nanotubes, nanofibers, and activated carbons are used in catalysts and adsorption fields due to their porous structure [2, 3].

When the literature was examined, it was seen that carbon-based materials (mesoporous carbon, carbon nanofiber, carbon nanospheres, carbon nanotube, activated carbon, graphene) are used as a support in many different reactions [4–20]. While Chen et al. were studied effects of promoters of K and Zr on the mesoporous carbon-supported cobalt catalysts for Fischer–Tropsch synthesis [4], Díaz et al. were used carbon nanofibers and nanospheres as support for cobalt and iron catalysts in order to use in the Fischer–Tropsch process [5–8]. Ubago-Perez et al. used carbon-supported Pt as catalysts for low-temperature methanol decomposition to carbon monoxide and hydrogen [9]. While Meng et al. used Ni/reduced graphene oxide catalysts for ammonia decomposition to hydrogen [10], Xuezhi et al. used carbon nanofiber supported Ru catalysts [11]. Li et al. used Ru/carbon nanotubes and Niu et al. used Ru/graphene-meso-macroporous SiO_2 composite for CO preferential oxidation in a H_2 -rich stream [12, 13]. Surisetty et al. used alkali promoted MoS_2 catalysts supported on multi-walled carbon nanotubes [14], and Kim et al. used ordered mesoporous carbon-supported uniform rhodium nanoparticles for higher alcohol synthesis from syngas [15]. Chen et al. used bimetallic cerium–copper nanoparticles embedded in ordered mesoporous carbons for the selective catalytic reduction of NO with NH_3 [16].

Donphaia et al. used Ni–CNTs/mesocellular silica composite catalysts for carbon dioxide reforming of methane [17]. Chiou et al. used Ni-doped ordered mesoporous carbon catalyst on the steam reforming of ethanol application [18]. Palacio et al. studied decomposition of ethanol into H_2 -rich gas and carbon nanotubes over Ni, Co and Fe supported on SBA-15 and Aerosil [19]. Jiménez et al. studied methanation over ruthenium carbon nanofibers catalysts [20]. In these studies, various metals were added to carbon supports as an active ingredient or as a second component to use less carbon economically, depending on the type of reaction designed. These metals were Co, Fe, Co–Fe, Pt, Ru, Ni, MoS_2 , Ce–Cu. When these metals were added to carbon supports, the most preferred method was the impregnation method. Most of the catalysts are commonly prepared by impregnation, in which the oxide support is contacted with a metal salt solution containing the desired metal. The different preparation methods have shown that the performance of the catalyst greatly depends on the synthesis methodology. Thus, the dispersion of the active phase, which will influence the accessibility of reagents, and the metal-support interaction, which often involves a synergistic effect important for a good catalytic performance, are strongly influenced by the method of preparation [21]. The homogeneous incorporation of active metal species onto the carbon matrix can be achieved by using impregnation [9]. The active phase is supported by high surface area oxides (SiO_2 , Al_2O_3 ...) mostly by either incipient wetness impregnation or slurry impregnation [5, 6].

As a result in this study, the metaloxide component was added to the porous structure of the carbon support using both impregnation and co-precipitation methods. Although CO methanation was examined in this study, since there are a limited number of carbon-assisted methanation studies in the literature, the studies on both CO_2 and CO methanation are summarized below. Multi-walled carbon nanotubes-supported mesoporous nickel catalysts were used for the carbon dioxide methanation by Wang et al. [22]. They used CeO_2 as a promoter, and results were compared with $\gamma\text{-Al}_2\text{O}_3$ -supported catalysts. They found that confinement effect of CNTs and the promotion effect of cerium efficiently prevented the migration of active species, sintering, and carbon deposition. Another significant property of cerium has stabilized the catalyst alongside deactivation due to more high temperature and more diffusion of the active metal [23]. Romero-Sáez et al. studied the CO_2 methanation over the nickel– ZrO_2 catalyst supported on carbon nanotubes. They investigated the effects of impregnation studies on the characteristic and catalytic properties [24]. Truszkiewicz et al. studied the effects of the preparation method on the CO methanation activities of Ru/graphitized-carbon catalysts. They obtained the complete conversion of CO to methane at $240 \text{ }^\circ\text{C}$ by using the graphitized carbon of appropriate structure in the preparation of the Ru/C catalyst [25]. Gödde

Table 1 Physical properties of the catalysts obtained from N₂ physisorption measurements

Catalysts	BET surface area m ² /g		Micro- + Mesopore volume (liquid N ₂ STP, cc/g)		Total pore volume (liquid N ₂ STP, cc/g)		% of meso- + micropore volume		Average pore diameter nm	
	CoP	Imp	CoP	Imp	CoP	Imp	CoP	Imp	CoP	Imp
Ni/MC	215	214	0.437	0.523	0.447	0.671	98.0	78.0	15.5, 46.3	9.4, 23.8
Ni/Gr	70	112	0.253	0.255	0.296	0.280	85.5	91.0	36.9	15.6
Ni/AC	219	108	0.300	0.246	0.321	0.266	93.5	92.5	5.2	9.4
Fe/MC	171	256	0.435	0.594	0.444	0.602	98.0	98.7	8.5	14.1
Fe/Gr	77.3	132	0.243	0.236	0.263	0.257	92.4	91.8	24.2	5.2
Fe/AC	268	219	0.419	0.305	0.439	0.321	95.4	95.0	9.2	3.2, 14.8
Co/MC	122	126	0.387	0.329	0.420	0.393	92.1	83.7	24.9	25.5
Co/Gr	62	50	0.279	0.219	0.317	0.258	88.0	85.0	15.3	27
Co/AC	78	72	0.334	0.211	0.386	0.239	86.5	88.3	24.7	9.3
MC	217		0.467		0.483		96.7		7,9	
AC	715		0.571		0.588		97.1		3.8, 4.9	
Gr	259		0.388		0.478		81.2		2.2, 3.8, 6.6, 9.4, 17.7	

*CoP: Co-precipitation, Imp: Impregnation
MC mesoporous carbon; Gr graphene oxide; AC activated carbon

et al. studied the CO₂ methanation over the nickel nanoparticles supported on nitrogen-doped carbon nanotubes. They found that optimum loading of 30–40 wt% Ni was found to result in the highest Ni surface area, the highest degree of conversion and the highest selectivity to methane [26]. Ahmad et al. studied the selective CO and CO₂ methanation over nickel catalysts supported on exfoliated graphitic carbon nitride with cerium (Ni–Ce/eg-C₃N₄) and lanthanum (Ni–La/eg-C₃N₄) as promoters. They obtained the high catalytic activity for CO₂ methanation by the enhancement of CO₂ adsorption and activation sites by the Ce promoter and eg-C₃N₄ support [27]. Xiong et al. studied the selective CO methanation over the carbon nanotube-supported Ru-based catalysts. They found that the metal promoter, reduction temperature, and metal loading have great effects on the catalytic properties. According to their results, amorphous and high dispersed Ru particles with small size were obtained for 30 wt% Ru–Zr/CNTs catalyst reduced at 350 °C which leads to excellent catalytic performance for CO selective methanation [28]. The aim of this study is to prepare different carbon type supported catalysts with different metaloxide additives with two different preparation methods and to test them for the CO methanation reaction. As a result of the literature research, it has been determined that there is a limited number of CO methanation studies in which carbon is used as a support. In this study, the effects of active ingredient type, support type, and preparation method on CO methanation were revealed.

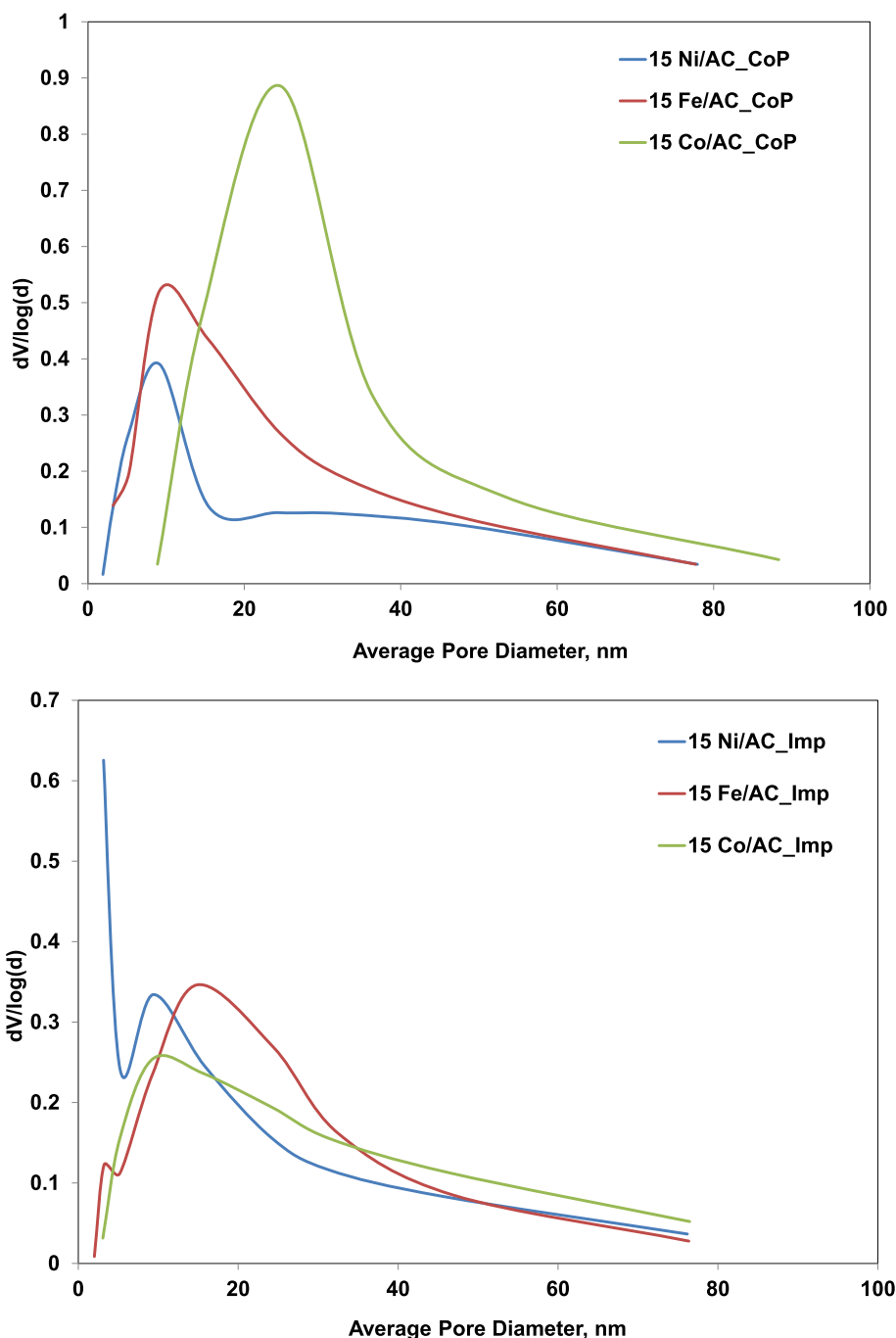
2 Experimental

In this study, nine types of catalysts were developed for the carbon monoxide methanation reaction using different metals, different carbon supports and two different preparation methods. NiO, Fe₂O₃, and Co₃O₄ were used as active component; graphene oxide, activated carbon, and mesoporous carbon were used as carbon support. All catalysts were prepared to contain 15 wt% Metaloxide/85 wt% carbon support. All catalysts were characterized to see the effects of the preparation method and support type on the physical properties of the catalysts. Afterward, all catalysts were tested for CO methanation reaction. The detailed procedure of the experimental is given below.

2.1 Catalyst Preparation

Co-Precipitation (CoP): The 85 wt% of the catalyst amount was carbon support by mass. This amount of carbon support (mesoporous carbon (Sigma-Aldrich), graphene oxide (Aldrich, powder 15–20 sheets), activated carbon (Merck)) and metal salts which are enough to form 15 wt% of metal oxide in catalyst composition (Ni(NO₃)₂·6H₂O (Sigma-Aldrich, 97%), Fe(NO₃)₃·9H₂O (Carlo Erba, 98%), Co(NO₃)₂·6H₂O (Sigma-Aldrich, 99%)) were mixed to prepare the catalysts at the desired mass composition. The

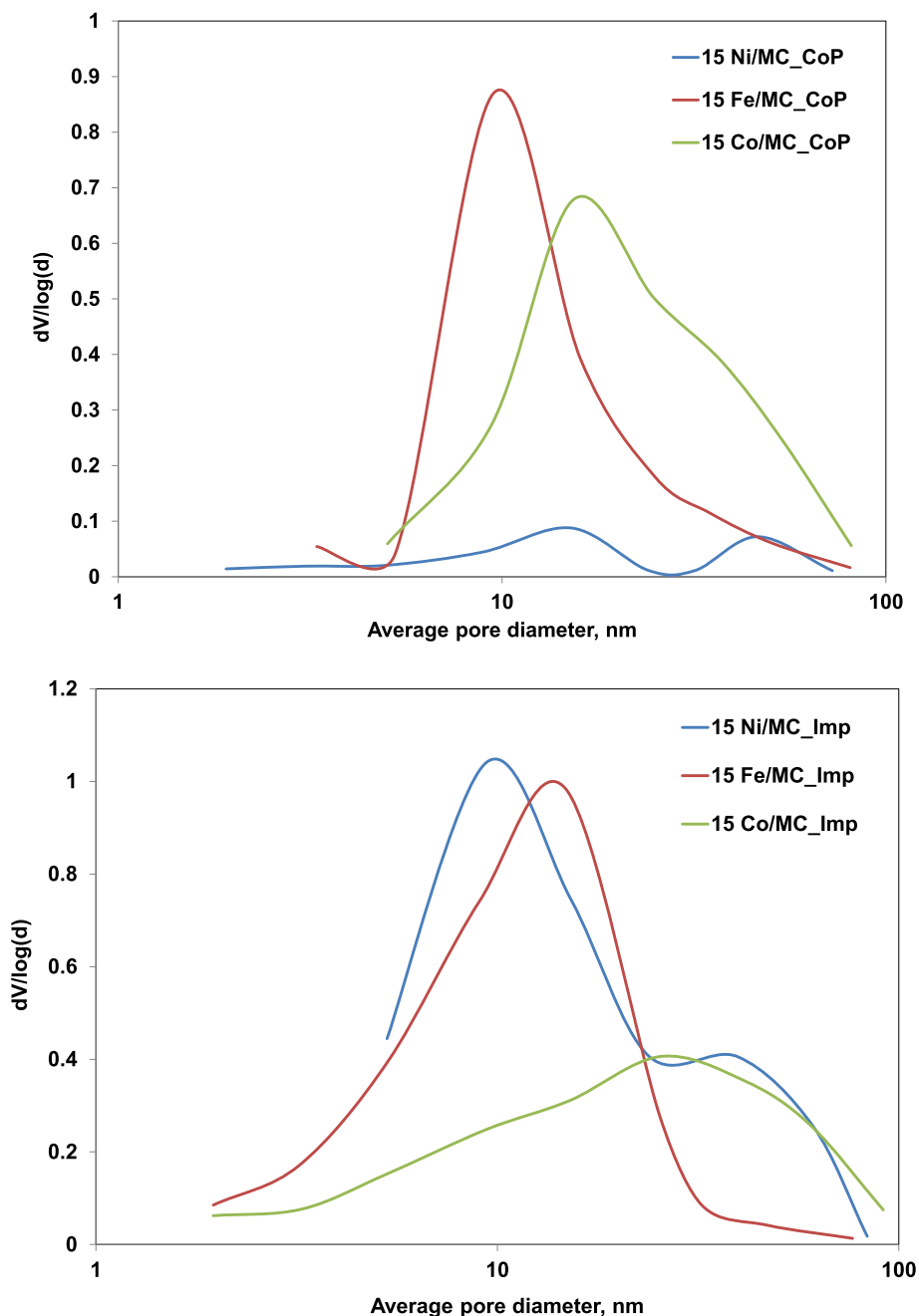
Fig. 1 Average pore diameter graphs of active carbon (AC)-supported catalysts



concentration of the metal salt solution was 0.1 M, which was prepared by using deionized water. In order to precipitate the metal salt solution, 1 M Na_2CO_3 solution was added dropwise (10 ml/min) to the prepared solution, which was mixed in the mixer, until the pH reached 8. The obtained solution was aged in a mixer for 3 h at room temperature. The solution was then filtered, washed with hot deionized water at 60 °C to remove excess ions, and dried at 110 °C for 12 h. The resulting catalyst was calcined at 350 °C for 3 h.

Impregnation (Imp): In this method, a solution with a low volume was prepared using deionized water, metal salts ($\text{Ni}(\text{NO}_3)_2 \cdot 6\text{H}_2\text{O}$ (Sigma-Aldrich, 97%), $\text{Fe}(\text{NO}_3)_3 \cdot 9\text{H}_2\text{O}$ (Carlo Erba, 98%), $\text{Co}(\text{NO}_3)_2 \cdot 6\text{H}_2\text{O}$ (Sigma-Aldrich, 99%), and carbon support [Mesoporous carbon (Sigma-Aldrich), graphene oxide (Aldrich, powder 15–20 sheets), activated carbon (Merck)], depending on catalyst composition. This mixture was aged by using the mechanical mixer at room temperature for 3 h. Then, for controlled drying, it was kept

Fig. 2 Average pore diameter graphs of mesoporous carbon (MC)-supported catalysts



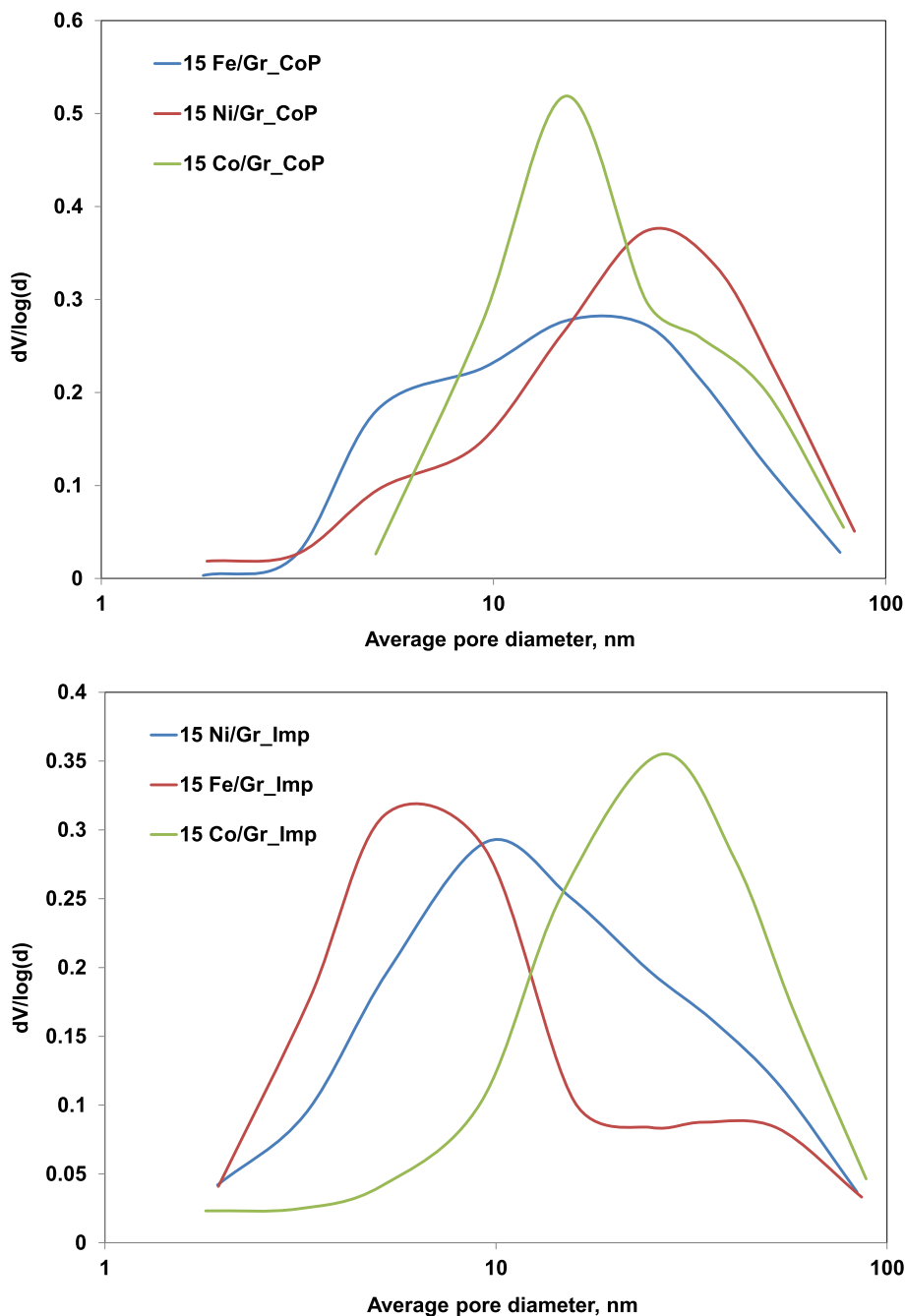
in an oven set at 40 °C for one day, and finally, the temperature of the oven was increased to 100 °C and dried at this temperature for one more night. Then, the obtained catalyst samples were crushed in a mortar and sieved. Finally, they were calcined at 350 °C for 3 h.

2.2 Catalysts Characterization

Different techniques are used to determine the physical properties of catalysts. These are X-ray diffraction

(XRD), N₂ physisorption, high-resolution transmission electron microscopy (HRTEM), scanning electron microscopy (SEM), and energy dispersion spectrometry (EDS) techniques. Multipoint surface areas, pore volumes, and pore diameters of the catalysts were determined in the Quantochrome Autosorp 1C/MS instrument. Before the analysis, the catalysts were degassed at 300 °C for 1 h. Average pore diameters were determined using the BJH method. X-ray diffraction patterns of the catalysts were determined in the PHILISPS PW 1840 diffractometer. Then XRD patterns were

Fig. 3 Average pore diameter graphs of graphene oxide (Gr)-supported catalysts



obtained on the Rigaku rotating anode X-ray diffractometry system producing $\text{CuK}\alpha$ radiation. Scanning electron microscopy (SEM) was used to analyze the surface properties and shapes of the particles. SEM measurements were performed on a Philips brand FEI/Quanta 400 F model device. JEOL JEM 2100F high resolution transmission electron microscope (HRTEM) with a maximum acceleration voltage of 200 kV was used for TEM analysis. The sample was prepared by dispersion in ethanol, and a drop of this suspension was deposited on a C-film covered grid. The

distribution of the components in the catalyst structure was determined by HRTEM analysis.

2.3 Catalytic Activity Measurements for CO Methanation

Catalytic activity tests of the catalysts were carried out in a fixed bed quartz reactor at atmospheric pressure and temperatures between 125 and 375 °C. A quartz reactor with a length of 70 cm, a thickness of 1 mm, and a diameter of 5 mm was

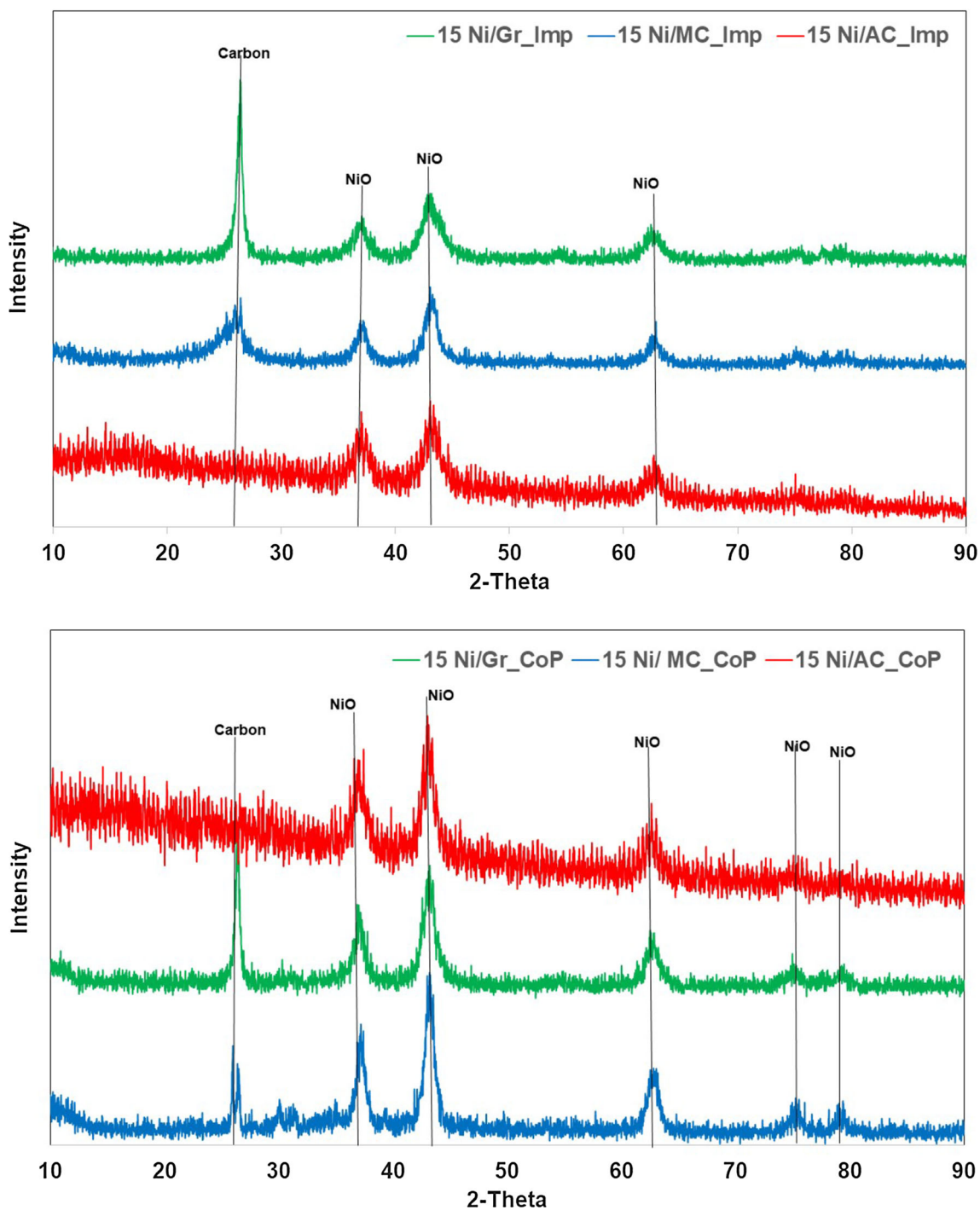


Fig. 4 X-ray diffraction patterns of different carbon-supported NiO composed catalysts

used. Before the reaction, the catalysts were reduced in situ with pure H₂ at 350 °C for 1 h. In order to prepare the feed gas the 10% vol. CO/90% vol. He, 100% vol. H₂ and 100% vol. He gases were used. The feed gas composition was 1% vol. CO, 50% vol. H₂ and 49% vol. He. Aalborg brand mass flow meters were used to prepare the feed gas mixture. Gas flow rates were calibrated by passing the gas from the mass

flow meter through a soap flow meter. The feed gas mixture was fed into the reactor at a total volumetric flow rate of 25 ml min⁻¹. According to the reactor dimensions and the total volumetric flow rate, the space velocity is 45,000 h⁻¹. The amount of catalyst was calculated from the space velocity and volumetric flow rate of the feed gas mixture. Some calculation steps were followed to determine the amount of

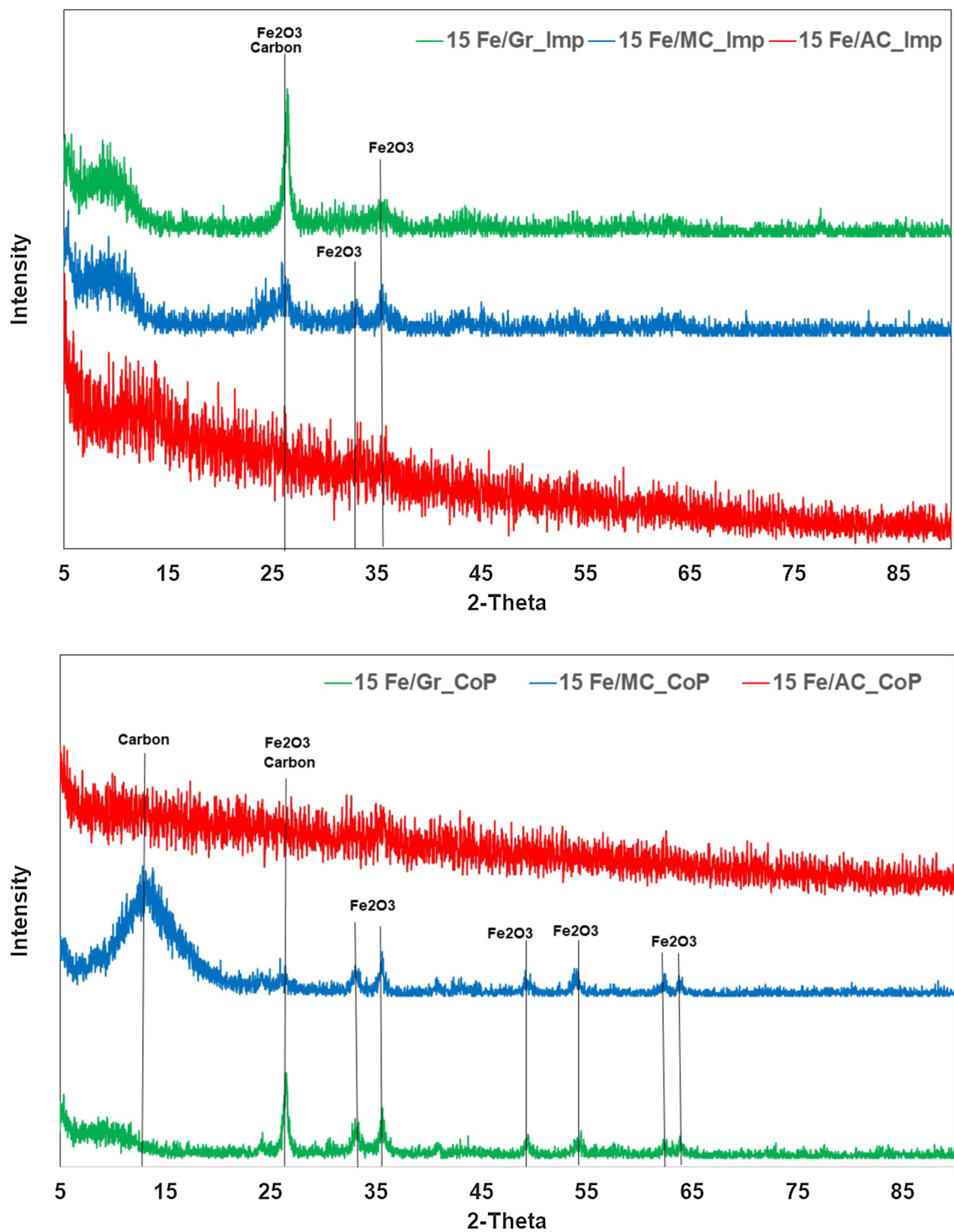


Fig. 5 X-ray diffraction patterns of different carbon-supported Fe₂O₃ composed catalysts

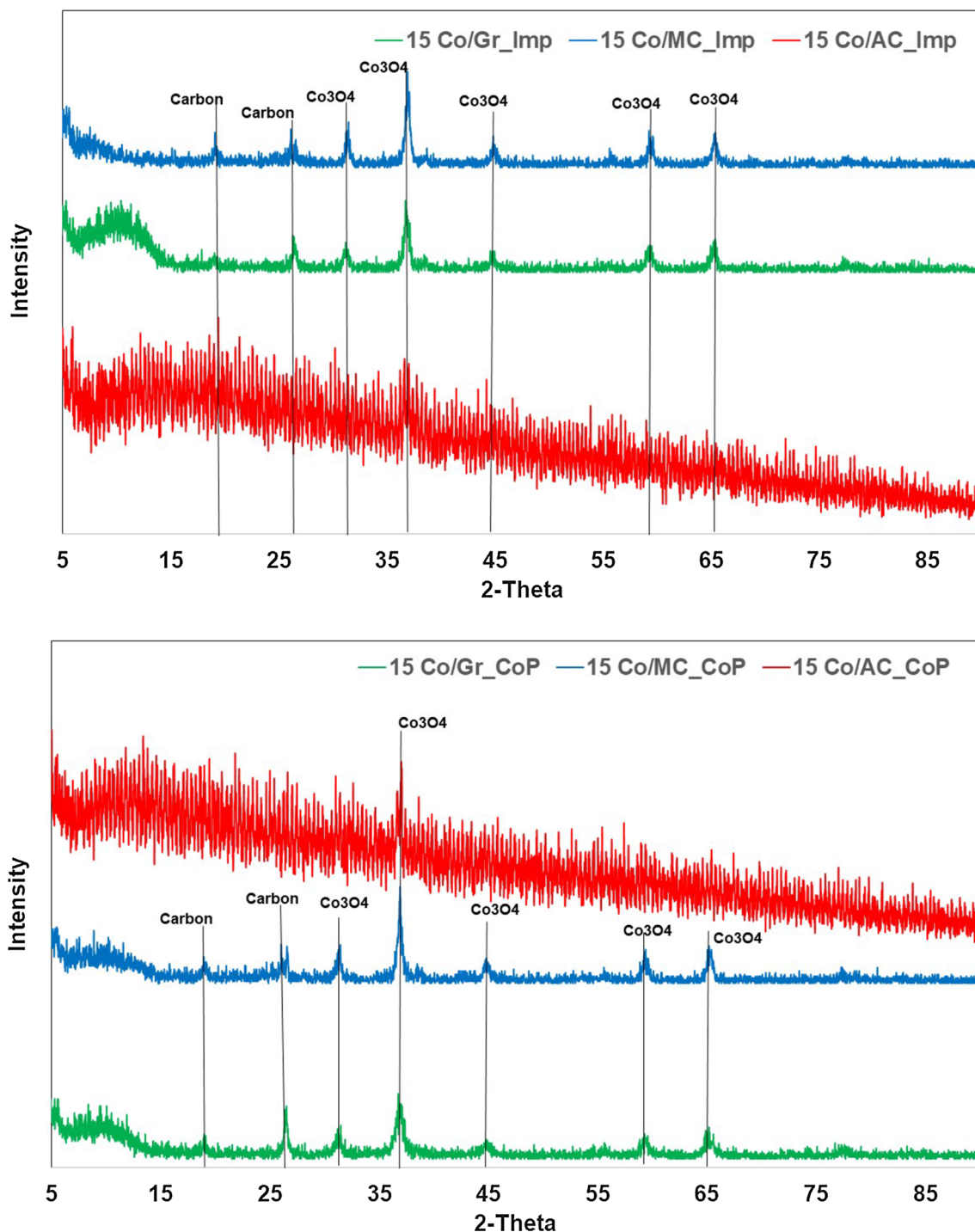


Fig. 6 X-ray diffraction patterns of different carbon-supported Co_3O_4 composed catalysts

catalyst. For this, the ratio of the volumetric flow velocity to the space velocity was first calculated. This value was then equalized to the volume of the reactor. As a result of this calculation, the reactor height to be filled with the catalyst was determined. All prepared catalysts have the same particle size as they are passed through a 150 mesh sieve.

Therefore, approximately 25 mg of prepared catalysts was sufficient to fill the calculated height. The catalyst was filled into the reactor from the top of the reactor, supported vertically by glass wool. At each reaction temperature at which the conversion of CO to methane was to be determined, at least 30 min was waited for the methanation reaction to stabilize

Table 2 Average crystal SIZES

Support	Average crystal size (Å)					
	NiO ($2\theta = 43.7^\circ$)		Co ₃ O ₄ ($2\theta = 37.1^\circ$)		Fe ₂ O ₃ ($2\theta = 35.7^\circ$)	
	CoP	Imp	CoP	Imp	CoP	Imp
MC	39.9	29.0	82.4	58.8	74.5	51.4
Gr	30.1	21.0	63.4	63.4	68.3	–
AC	26.3	26.3	–	–	–	–

in the catalyst bed. Then, the reaction product composition was analyzed when the product analysis result was obtained at least three times in a row in gas chromatography. Feed and product gas compositions were analyzed by gas chromatograph (CLARUS 500, PerkinElmer) equipped with a thermal conductivity detector (TCD) with a separation column filled with carbosphere. In order to make the separation of hydrogen, carbon monoxide, methane, and carbon dioxide gas components correctly, 50 °C temperature was chosen as the column temperature from the carbosphere operating temperatures. Detector temperature was determined as 125 °C.

The CO conversion was calculated using the equation given below.

$$\% \text{ CO Conversion} = \frac{[\text{CO}]_0 - [\text{CO}]_f}{[\text{CO}]_0} \times 100$$

Here $[\text{CO}]_0$ is the amount of CO in the feed, and $[\text{CO}]_f$ is the amount of unreacted CO in the product stream. The concentration of methane in the product was determined by the calibration calculations made as a result of the analysis of 1% vol. CH₄/99% vol. He mixture before the activity tests.

3 Results and Discussion

3.1 N₂ Physisorption Results

The surface area results of the catalysts are shown in Table 1. The highest surface area values were obtained in catalysts containing both mesoporous carbon and graphene oxide supported Fe catalysts. When the surface area results were examined in terms of the preparation method, the catalysts prepared by the impregnation method gave higher surface area values. When the surface area results were examined depending on the carbon support type, it was determined that the activated carbon- and mesoporous carbon-supported catalysts gave higher surface area results. The surface area of activated carbon alone was of great value. It can be seen from Table 1 that the surface areas of activated carbon-supported catalysts were much lower than the surface area value of activated carbon alone as a result of the addition of metal oxides

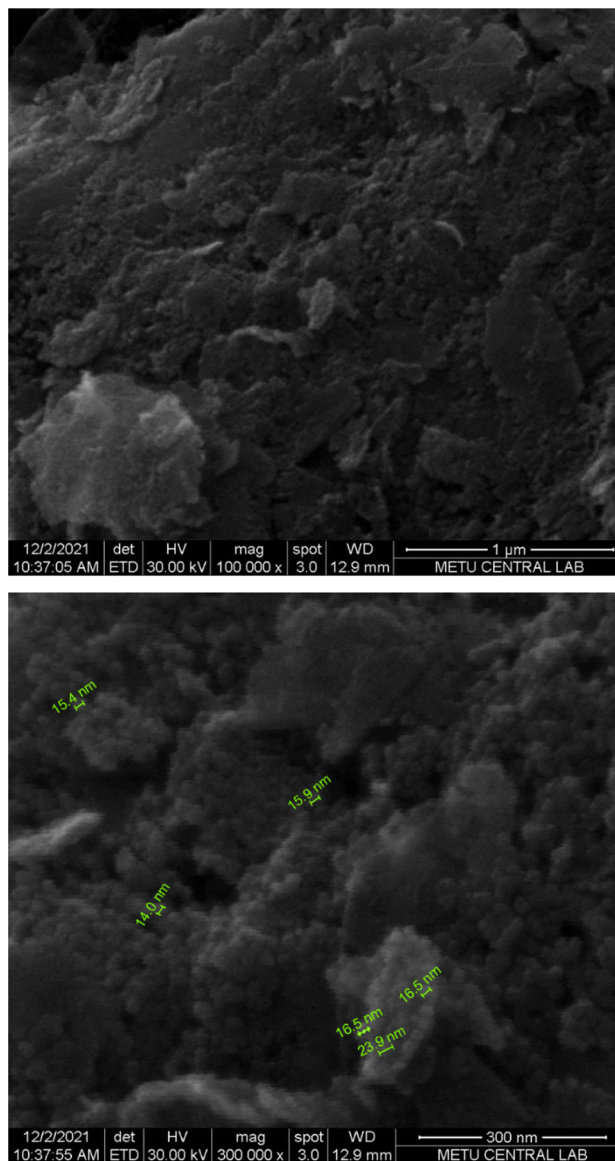


Fig.7 SEM photograph of Co₃O₄/graphene oxide prepared by impregnation method

to the structure and the applied heat treatment. Similar to activated carbon, the surface areas of graphene oxide supported catalysts were also obtained lower than the surface area value of graphene oxide alone. The decrease in this surface area in

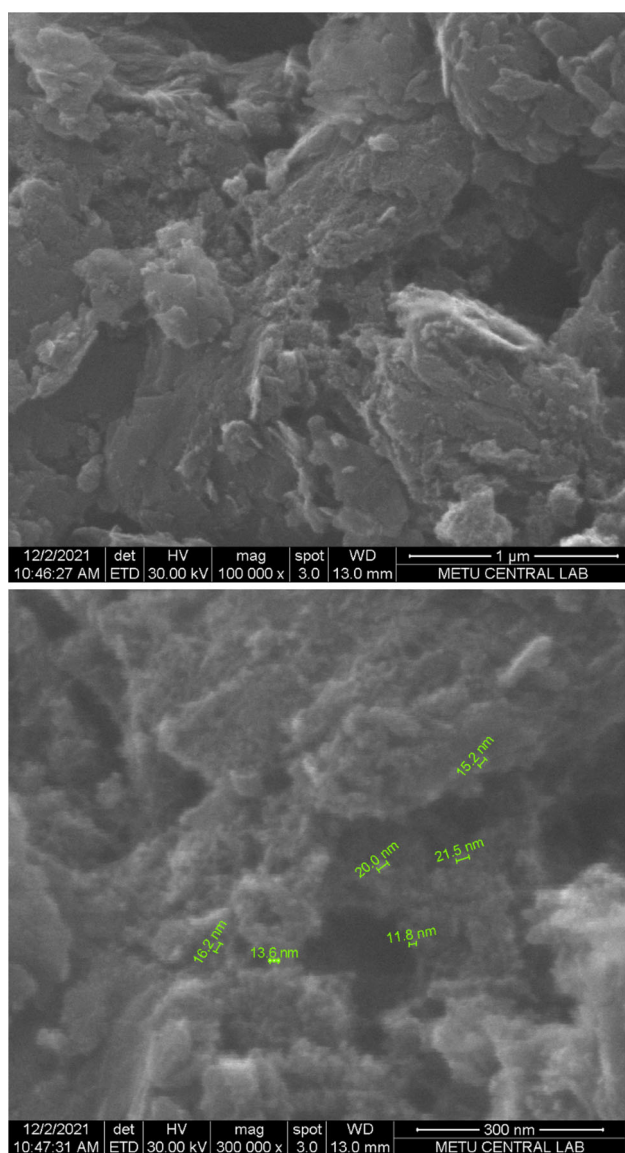


Fig. 8 SEM photograph of Co_3O_4 /graphene oxide prepared by co-precipitation method

graphene oxide-supported catalysts was not as low as in activated carbon-supported catalysts. In the surface area value, the least loss according to the surface area of the support was observed in the mesoporous carbon-supported catalysts. This decrease indicates that the metal oxide component has entered the porous structure and may have resulted from the conversion of some carbon into CO_2 as a result of calcination under weather conditions.

The total pore volume (Micropore + Mesopore + Macropore) results and micropore + mesopore volume values of the catalysts prepared are shown in Table 1. By comparing the total pore volume values with the mesopore + micropore volume values, it was determined that the macropore volume values in the structure of the catalysts were low.

According to this result, mesopore + micropores are mostly present in the structure of the catalysts. Parallel to the surface area results, both total pore volume values and mesopore + micropore volume values were higher in mesoporous carbon-supported catalysts prepared by impregnation method. In the catalysts prepared by both methods in graphene oxide supported catalysts, both pore volume values were obtained low. According to the values given in Table 1, it was determined that the catalysts had varying pore diameter values within the scale of mesoporosity ($2 \text{ nm} < d_{\text{ave}} < 50 \text{ nm}$). When Figs. 1, 2, 3 are examined, it is seen that the area under the mean pore diameter curves is wide (not narrow, thin). According to this result, it is understood that there are many different size pores in the structure of the catalysts and the pore diameter values are focused on the values given in Table 1. The adsorption/desorption isotherms of the catalysts are similar to Type V in the Brunauer–Deming–Deming–Teller (BDDT) classification. Type V occurs in mesoporous solids. Adsorption takes place first, followed by capillary condensation. The characteristic feature of this type of isotherm is the Hysteresis Range. The hysteresis range is due to capillary condensation in the mesopores. In addition, H3 Type hysteresis range was seen in the catalysts. The H3 Type hysteresis range indicates that there are particles in the structure that form slit-like pores, and H3 hysteresis loop is typical of porous materials [29].

3.2 X-ray Diffraction Results

X-ray diffraction analyses were done to determine the crystal phases present in the catalysts. X-ray diffraction patterns of catalysts are given in Figs. 4, 5, 6. The most intensive diffraction peaks of NiO crystal phase were observed at $2\theta = 37.1^\circ, 43.3^\circ, 62.5^\circ, 75.6^\circ, 79.2^\circ$ (JCPDS card no = 47–1049) (Fig. 4). The diffraction peaks due to the $\alpha\text{-Fe}_2\text{O}_3$ crystal phase (JCPDS card no = 33–0664) were observed at $2\theta = 32.9^\circ, 35.4^\circ$ from catalysts prepared by impregnation method and at $2\theta = 32.9^\circ, 35.4^\circ, 49.2^\circ, 54.4^\circ, 62.3^\circ, 63.9^\circ$ from catalysts prepared by the co-precipitation method (Fig. 5). The Co_3O_4 crystal phase (JCPDS card no = 42–1467) diffraction peaks were observed at $2\theta = 31.2^\circ, 37.1^\circ, 44.8^\circ, 59.2^\circ, 65.7^\circ$ diffraction angles. The carbon diffraction peak due to the graphene oxide support was obtained at $2\theta = 26^\circ$, which is well-matched with JCPDS card no = 41–1487 [30]. Except for 15 Ni/AC catalysts, all other activated carbon-supported catalysts showed amorphous crystal phase structure. The diffraction peaks due to the carbon phase from the activated carbon-supported catalysts can be supported by other studies. Wibawa et al. [31] conducted SEM, XRD and FTIR studies over the activated carbon microstructure. They observed three diffraction peaks between $5^\circ\text{--}10^\circ, 20^\circ\text{--}30^\circ$ and $40^\circ\text{--}50^\circ$ angles. Aravind et al. [32] observed the diffraction peaks from the country egg shell

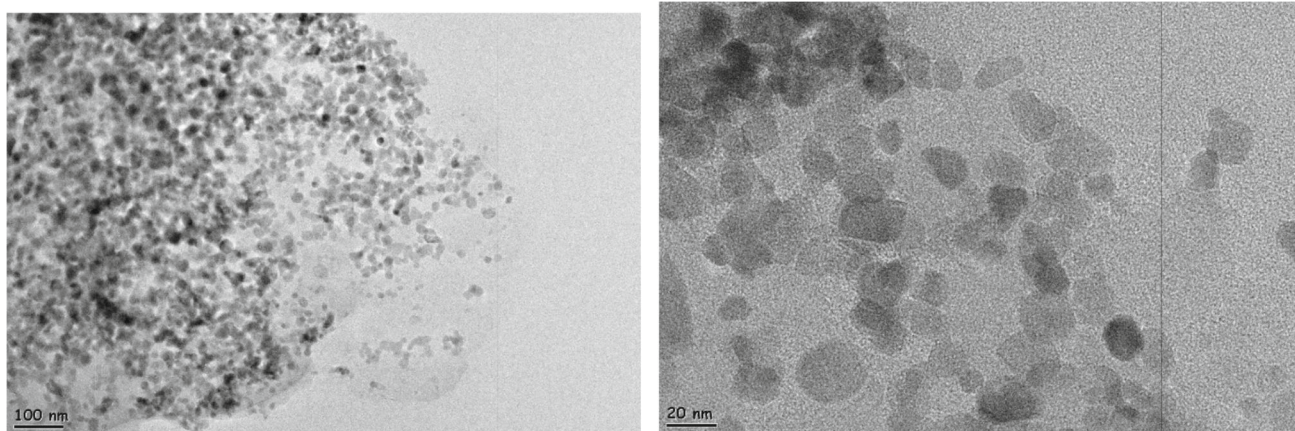


Fig. 9 HRTEM photograph of Co_3O_4 /graphene oxide prepared by impregnation method

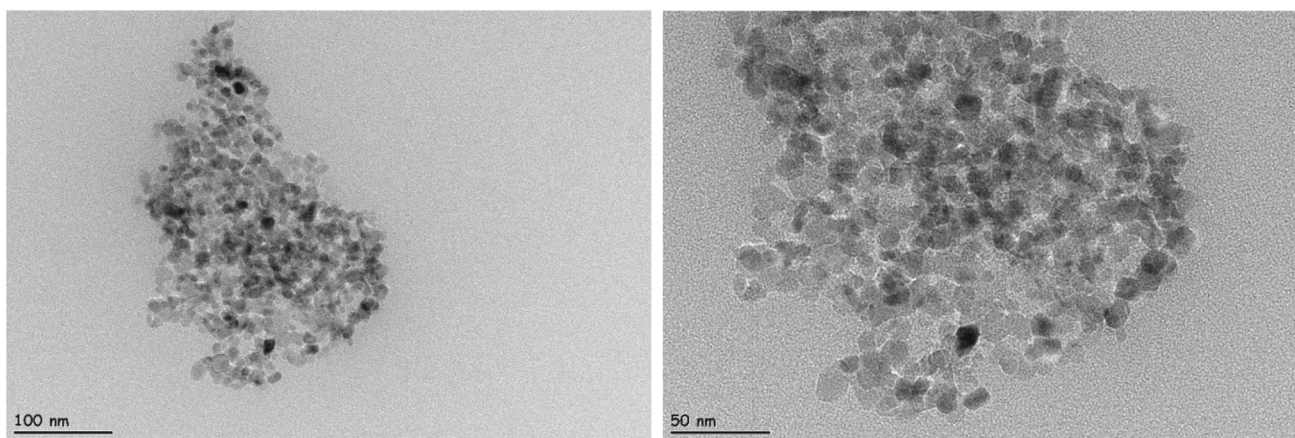


Fig. 10 HRTEM photograph of Co_3O_4 /graphene oxide prepared by co-precipitation method

derived activated carbon sample at $2\theta = 20.48^\circ, 23.54^\circ, 25.18^\circ, 27.29^\circ, 29.29^\circ, 31.60^\circ, 33.59^\circ, 36.16^\circ$ and 46.37° angles. Among them, the most intensive peak was observed at $2\theta = 25.18^\circ$. However, in our study, the diffraction peak of the carbon crystal phase originating from activated carbon was not found at the reflection angles specified in the literature. Table 2 shows the average crystal sizes of the catalysts. The smallest crystal sizes were obtained from carbon-supported catalysts containing nickel oxide. It was seen that the average crystal sizes increase when the catalysts were prepared by the co-precipitation method. When the table is examined in general, it has been determined that the largest crystals are generally in cobalt-oxide-containing catalysts. Since the catalysts containing activated carbon-supported cobalt-oxide and iron oxide and the graphene oxide-supported iron oxide-containing catalysts prepared by the impregnation method showed amorphous crystalline phase, average crystal size values for these catalysts could not be calculated.

3.3 Electron Microscopy Analysis Results

Since the total conversion of carbon monoxide was obtained from the Co_3O_4 /Graphene oxide catalyst at the lowest temperature, SEM and HRTEM studies were carried out on this catalyst. In order to see the effect of the preparation method, the images of the catalysts prepared by both methods were compared.

3.3.1 Scanning Electron Microscopy (SEM) Results

Figures 7 and 8 show the surface morphologies of the Co_3O_4 /graphene oxide catalysts prepared with both two methods, which are co-precipitation and impregnation obtained from scanning electron microscopy. On the surface of the catalysts, spherical particles on the planar particles were formed. The size of the spherical particles were much less smaller in the catalyst prepared by the co-precipitation

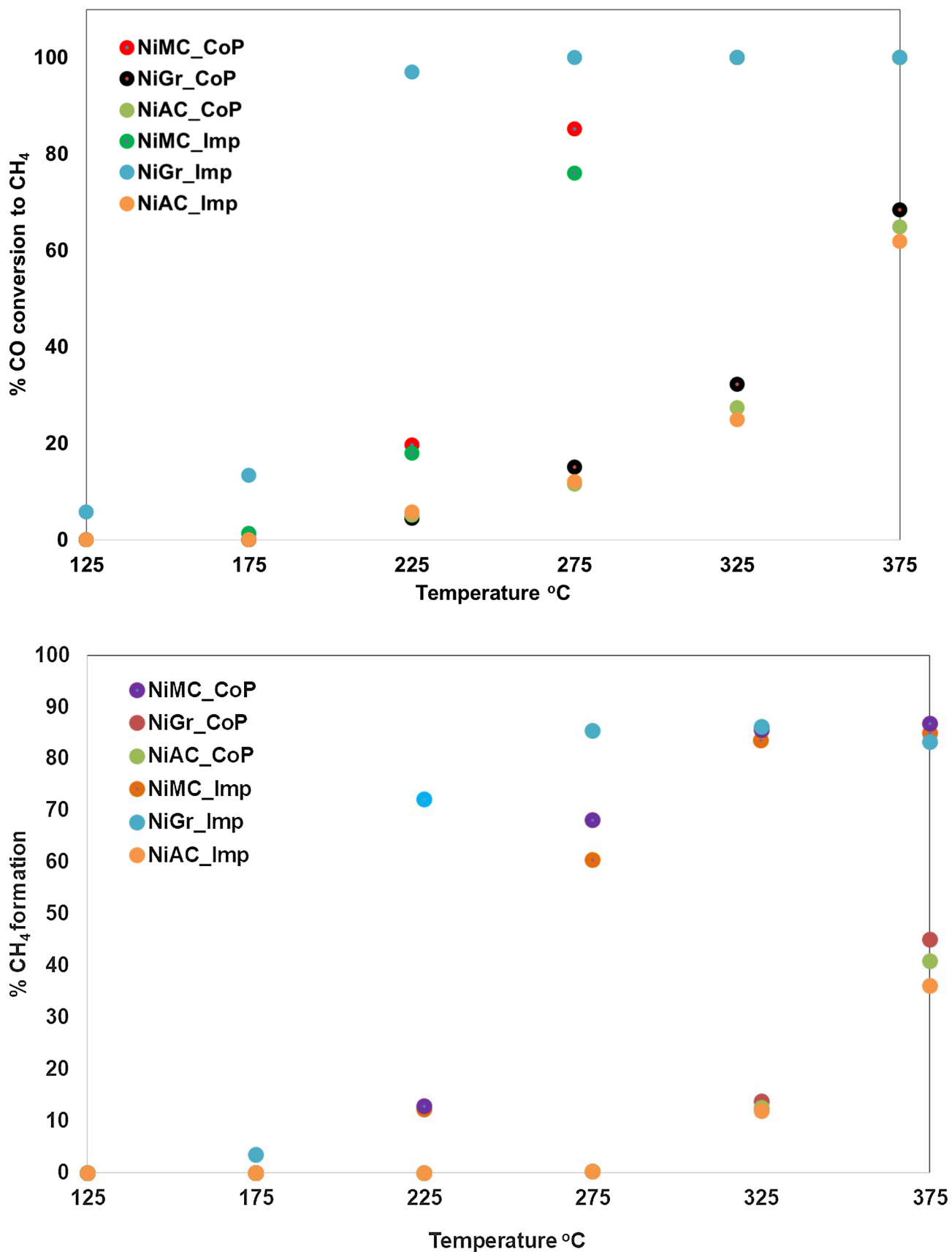


Fig. 11 Methanation activity results obtained over the nickel composed catalysts (Feed composition: 1% vol. CO, 50% vol. H₂, 49% vol. He; 25 mg catalysts, flow rate 25 ml min⁻¹)

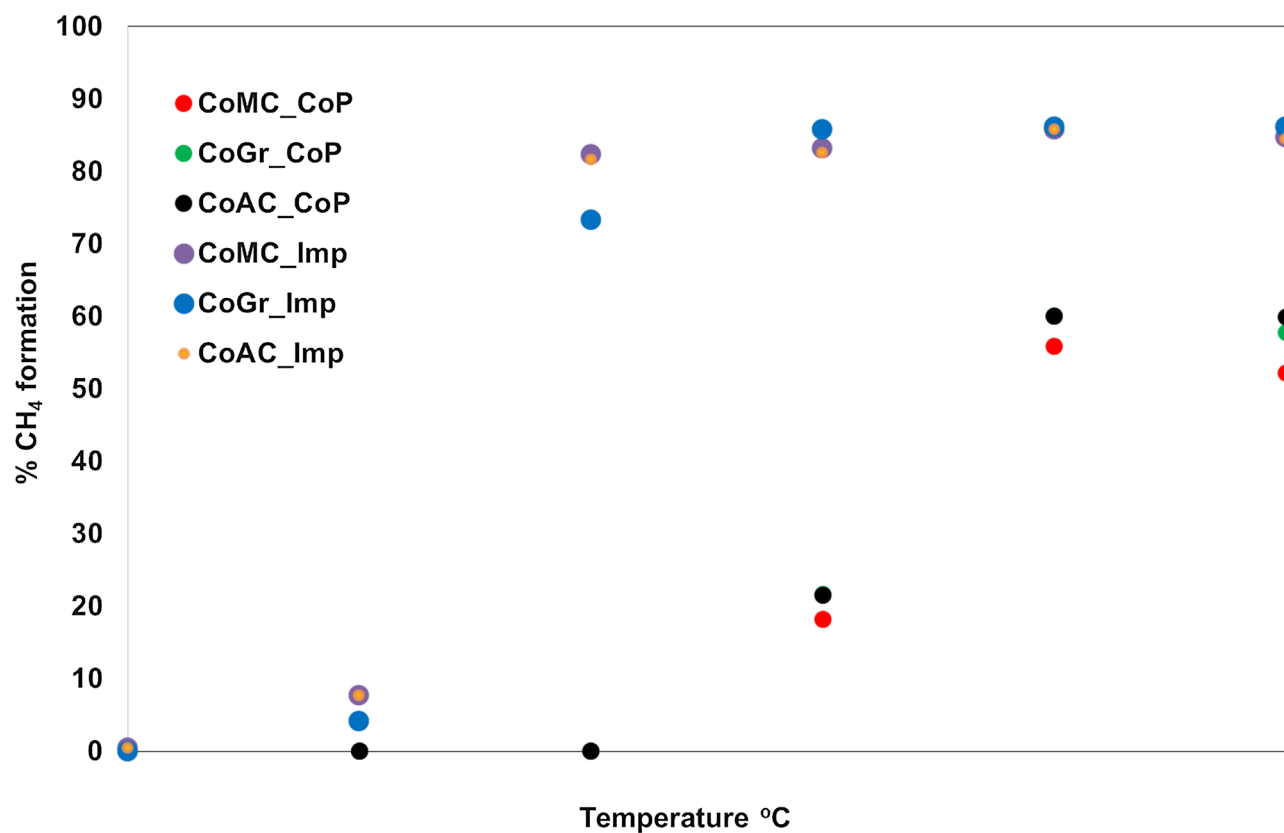
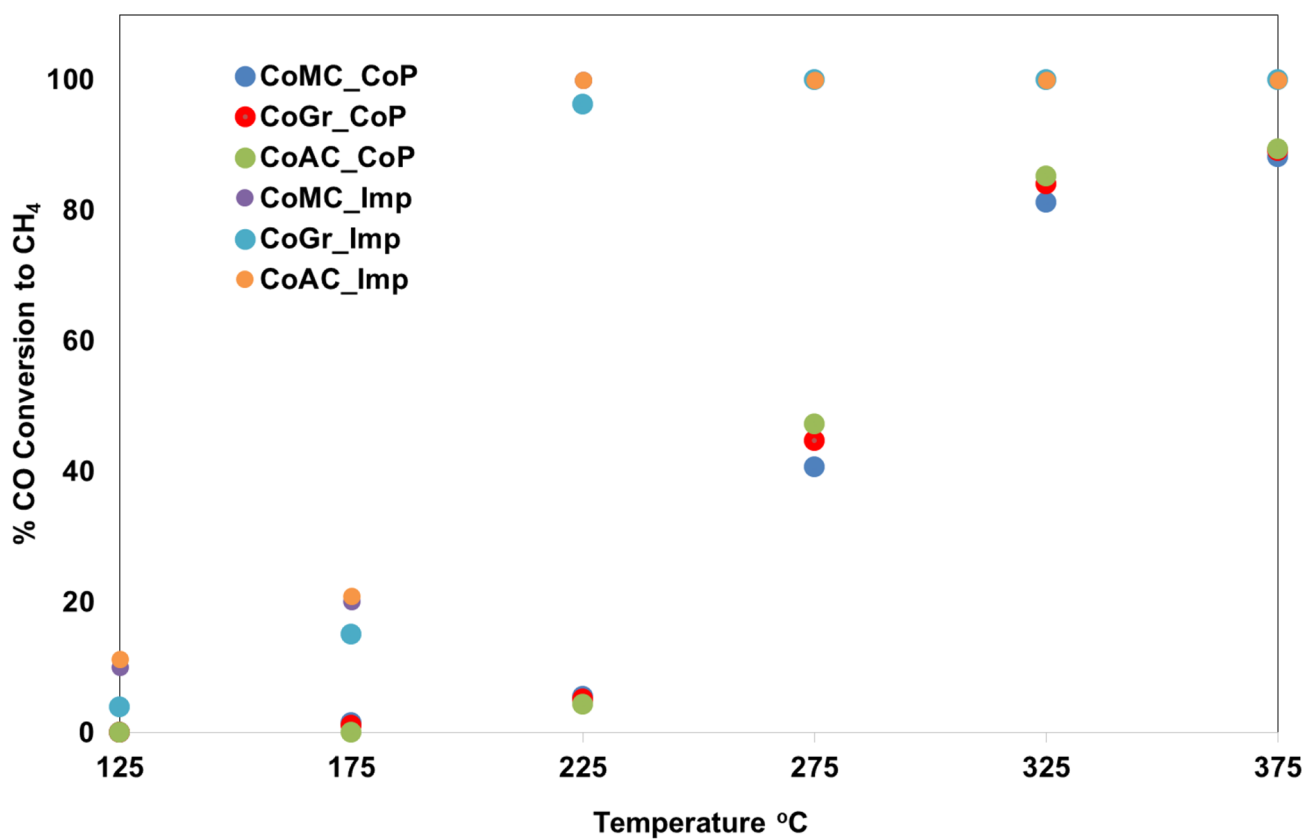


Fig.12 Methanation activity results obtained over the cobalt composed catalysts (Feed composition: 1% vol. CO, 50% vol. H₂, 49% vol. He; 25 mg catalysts, flow rate 25 ml min⁻¹)



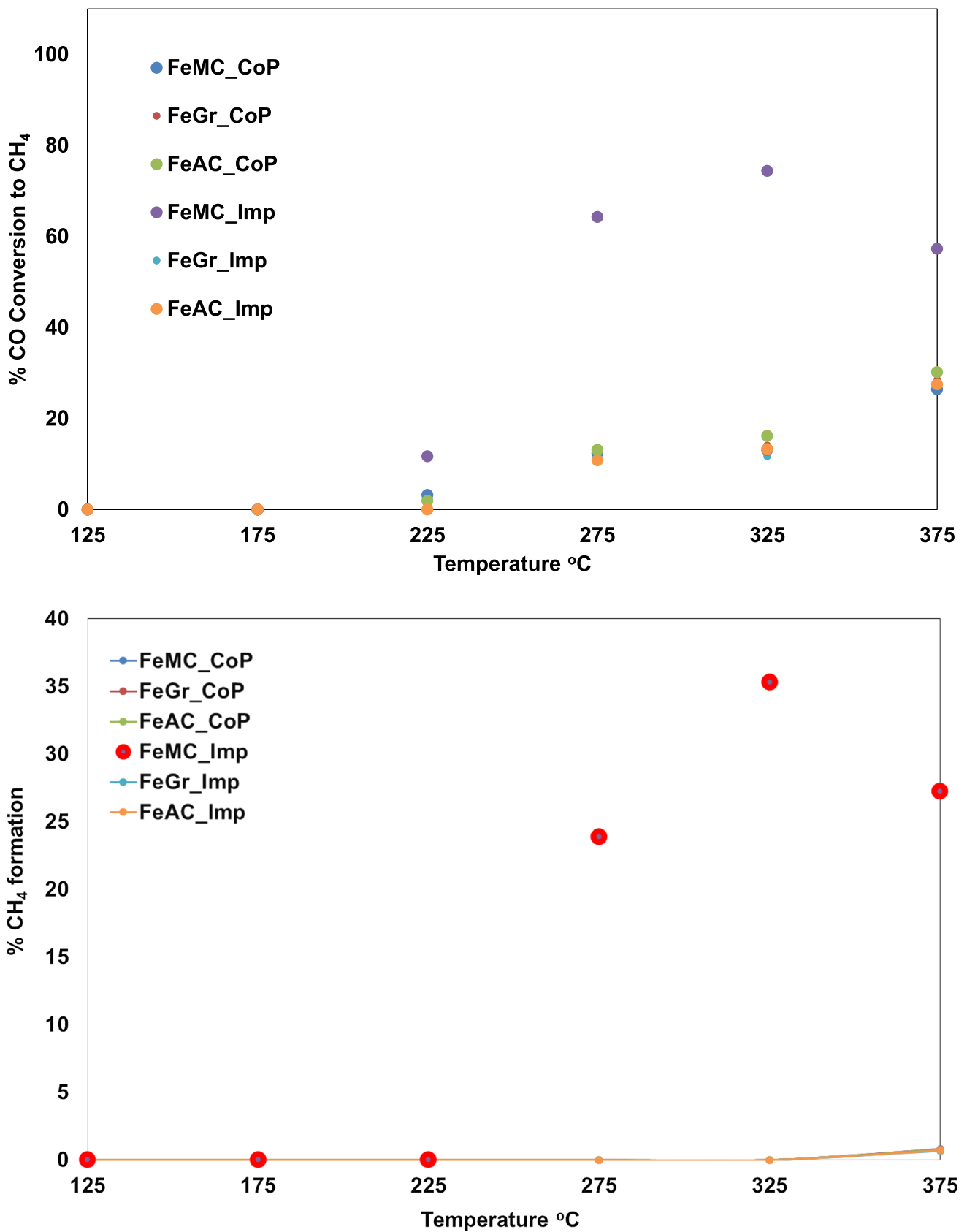


Fig.13 Methanation activity results obtained over the iron composed catalysts (Feed composition: 1% vol. CO, 50% vol. H₂, 49% vol. He; 25 mg catalysts, flow rate 25 ml min⁻¹)

method. While the average particle size was 17.3 nm for the catalyst prepared by the impregnation method, the average particle size was 16.4 nm for the catalyst prepared by the co-precipitation method. SEM images shows that the porous structure of graphene oxide mixes with Co_3O_4 in nanostructures [33].

3.3.2 High Resolution Transmission Electron Microscopy (HRTEM) results

Figures 9 and 10 show the high-resolution transmission electron microscopy images of the Co_3O_4 /graphene oxide catalysts prepared with both methods which are co-precipitation and impregnation. Black areas show the metaloxide particles. This result shows us that Co_3O_4 particles have entered the pores. Homogeneous distribution of metaloxide particles was observed. The formation of GO sheets and spherical-shaped Co_3O_4 grains were clearly observed in the HRTEM images of the Co_3O_4 /Graphene oxide catalysts. It was clearly seen that the Co_3O_4 particles penetrated into the GO leaves [33].

3.4 Catalytic Activity Results

In this study, carbon monoxide methanation was carried out over the catalysts which were composed of three different active components, which were NiO, Co_3O_4 , Fe_2O_3 supported on different type carbon [activated carbon (AC), mesoporous carbon (MC), graphene oxide (Gr)]. The chemical conversion of three hydrogen moles and one carbon monoxide mole into one mole of methane and one mole of water is known as CO methanation or CO hydrogenation [$\text{CO} + 3\text{H}_2 \leftrightarrow \text{CH}_4 + \text{H}_2\text{O}$]. It is achieved between 300 and 550 °C at 1 to 100 bars in the presence of an effective catalyst. During the stoichiometric reaction of CO methanation, 206.28 kJmol^{-1} (2.3 kW) heat and 1 m^3 methane are produced per hour, confirming a highly exothermic reaction [34]. Catalysts were prepared by using impregnation and co-precipitation methods. Activity studies showed us the results of the effects of active component, effects of preparation methods and effects of carbon support type on the conversion of carbon monoxide to methane. In order to determine the accuracy in the activity results and to determine that the conversion values were taken at equilibrium, the tests were repeated three times at each temperature and it was decided that the obtained conversion results were the result of the equilibrium conversion at that temperature. Activity results are given between Fig. 11 and Fig. 13. The different carbon type supported Co_3O_4 catalysts prepared by using the impregnation method had the lowest 50% CO conversion temperature. As can be seen in Table 3, these catalysts have a 50% conversion temperature lower than 200 °C. NiO/graphene oxide catalyst synthesized by the impregnation method showed the same good activity

Table 3 50% CO conversion temperature to CH_4 of the catalysts

Catalysts	Preparation method		
	Support	Co-precipitation	Impregnation
Ni	MC	246 °C	251 °C
	Gr	249 °C	198 °C
	AC	355 °C	358 °C
Co	MC	286 °C	195 °C
	Gr	281 °C	197 °C
	AC	278 °C	195 °C
Fe	MC	–	259 °C
	Gr	–	–
	AC	–	–

as cobaltoxide-containing catalysts (50% conversion yield temperature 198 °C). When the activities were evaluated in terms of method, the catalysts prepared by the impregnation method had higher activity. When activities were evaluated in terms of active component (metaloxide) type, cobalt oxide active component provided better results.

When the activities were evaluated in terms of support type, higher activities were obtained from the graphene oxide supported catalysts (except Fe_2O_3). Among the different carbon type catalysts containing NiO, graphene oxide synthesized by the impregnation method and mesoporous carbon-supported catalysts and the mesoporous carbon-supported catalyst synthesized by the co-precipitation method had the highest activity ($\text{Ni/Gr_Imp} > \text{Ni/MC_CoP} > \text{Ni/MC_Imp}$) (Fig. 11). Other nickel oxide-containing catalysts were able to achieve 50–60% CO conversion at a maximum reaction temperature of 375 °C. Between NiO-containing catalysts, the best activity was obtained over NiO/graphene oxide synthesized via impregnation, NiGr_Imp. When the activity results and the characterization results are interpreted together, a direct relationship cannot be established even though the catalysts with the highest surface areas in the nickel oxide-containing catalyst show the best catalytic activity. Although the nickel oxide-containing activated carbon-supported catalyst prepared by the co-precipitation method had a high surface area, it did not show high catalytic activity. Although there is no linear relationship between the catalyst surface area and the catalytic activity, there is a relationship with the average crystal size of the active ingredient in the catalyst structure. Among the catalysts containing NiO, the highest catalytic activity was obtained from the catalyst with the smallest NiO average crystal size (Table 2). The small average crystal size of NiO may have caused the NiO crystals to be homogeneously dispersed in the porous structure and not agglomerate. This may have caused the catalyst to give high activity.

Table 4 Methanation studies over the carbon-supported catalysts

Authors	Reaction	Catalysts	Results	Ref. No
Jimenez et al.	CO and CO ₂ methanation were studied	Carbon nanofiber-supported Ru catalysts	At 340 °C all CO converted to CH ₄ Orientation of graphite planes affects the catalytic activity	[37]
Variava et al.	CO methanation	Ni/multiwall carbon nanotubes	95% CO conversion and 85% CH ₄ selectivity were observed at 400 °C	[38]
Truszkiewicz et al. (2020)	CO methanation	Ru/graphitized-carbon	100% CO conversion observed at 240 °C Activities of the catalysts depends on structure and average size of the active phase crystallites	[25]
Gonçalves et al.	CO ₂ methanation	Ni/activated carbon	Methanation reaction is highly dependent on the basicity of the support 76% CO ₂ conversion, 97% CH ₄ selectivity were obtained at 450 °C	[39]
Xiong et al.	CO selective methanation	Ru/carbon nanotube	Metal promoter, reduction temperature and metal loading affected the catalytic properties 30 wt% Ru–Zr/CNTs catalyst was Show excellent catalytic performance between the 180 – 240 °C reaction temperature	[28]
Ahmad et al.	Selective CO and CO ₂ methanation	Ni/exfoliated graphitic carbon nitride Ni–Ce/exfoliated graphitic carbon nitride Ni–La/exfoliated graphitic carbon nitride	The promoted catalysts showed an increased number of mesopores, a higher degree of dispersion of Ni nanoparticles, moderate metal-support interaction, and more surface basic sites Ni–Ce/eg–C ₃ N ₄ catalyst exhibited the best CO methanation (72% CO conversion, 89% CH ₄ selectivity at 279 °C) (83% CO ₂ conversion and 99% CH ₄ selectivity at 297 °C)	[27]

Among the catalysts containing cobalt oxide, the best activity results were generally obtained from the catalysts synthesized by the impregnation method (Fig. 12). Also, 100% CO conversion was obtained over these catalysts after 225 °C. Compared to other catalysts, approximately 85% CO conversion was obtained after a maximum temperature of 325 °C over different carbon-type catalysts containing cobalt oxide synthesized by the co-precipitation method. Catalysts prepared by the impregnation method in different carbon type supported catalysts containing cobalt oxide showed better catalytic activities. When the activity results and surface area results were interpreted together, better activity results were obtained from cobalt oxide-containing catalysts, although lower surface area values were obtained

than other catalysts. Based on this result, it can be concluded that the active component, which is more in the structure than the surface area, is effective in obtaining high catalytic activity. Cobalt oxide-containing carbon-supported catalysts prepared via impregnation have lower average crystalline size than catalysts prepared via co-precipitation. Among these catalysts, the small average crystal size was also effective in obtaining high catalytic activity.

Fe₂O₃-containing catalysts gave very low activity results compared to other NiO and Co₃O₄-containing catalysts (Fig. 13). Among the Fe₂O₃-containing catalysts, the mesoporous carbon-supported catalyst synthesized by the impregnation method showed the best catalytic activity result. With this catalyst, 65–70% CO conversion was obtained at 325 °C.



When Table 1 is examined, it can be seen that the catalysts with high surface area are generally those containing Fe_2O_3 . Therefore, there is no direct relationship between surface area and activity in this study. Activity studies have shown that the preparation method and type of active component are effective in obtaining high catalytic activity. The best activity results were obtained from the catalysts synthesized by the impregnation method and the catalysts containing cobalt oxide. In Table 2, it is seen that the mesoporous carbon-supported Fe_2O_3 catalyst prepared by the impregnation method has the smallest average crystal size. In catalysts containing Fe_2O_3 , the activity was also obtained on the catalyst with a small average crystal size. Therefore, it is seen that the average crystal size of the catalyst active component is effective on the CO methanation catalytic activity. Higher activity is obtained on the catalyst with small crystals.

Although the CO conversion is important for the methanation reaction, it is also very important how much of this converted carbon monoxide is converted to the methane component, which is the reaction product. In Fig. 11, the CH_4 formation obtained over nickel oxide-containing catalysts can be seen depending on the reaction temperature. The highest methane formation was obtained from graphene oxide-supported catalyst synthesized by the impregnation method. Subsequently, mesoporous carbon-supported catalysts prepared by both methods showed similar high methane formation. Over 80% CH_4 formation was achieved. This result shows that the most of the carbon monoxide is converted to methane. After 375 °C, a maximum of 45% methane formation was obtained from other nickel oxide-containing catalysts. In Fig. 12, the CH_4 formation obtained over cobalt oxide-containing catalysts can be seen. They have a maximum of 85–90% CH_4 formation from catalysts containing cobalt oxide synthesized by the impregnation method. This result shows that most of the CO is converted to CH_4 . From other cobalt oxide-containing catalysts, approximately 50–60% CH_4 formation was obtained at a maximum temperature of 325 °C. Figure 13 shows the CH_4 formation obtained over carbon-supported catalysts containing Fe_2O_3 . The highest value was obtained with the mesoporous carbon-supported Fe_2O_3 catalyst prepared by the impregnation method at 325 °C with the formation of 33% CH_4 . When this result is compared with the CO conversion results, it shows that about half of the CO is converted to methane. In other Fe_2O_3 -containing catalysts, methane formation was obtained below 3% (375 °C). It has been stated in the literature that catalysts containing iron oxide do not show high activity for CO methanation. Kang et al. studied CO methanation of CO and CO_2 over the $\text{Ni}_X\text{-Fe}_{1-X}/\text{Al}_2\text{O}_3$ catalysts and observed that high Fe content caused a decrease in carbon conversion and CH_4 productivity because of WGS reaction [35]. Derekaya et al. studied the CO methanation over the NiFeSi

mixed oxide catalysts and indicated that reaction would prefer the catalyst with low Fe and Si ratio and high Ni ratio because activity was increased by decreasing Fe content in the catalysts structure [36].

The behavior of catalysts that show activity for CO methanation can be related to the crystal sizes in their structures. In the case where the active ingredient type is constant and the support changes, the catalytic activity is higher than the catalyst with the smallest crystal size, while higher catalytic activity is obtained from the catalyst with the higher average crystal size according to the type of active ingredient. It is seen from Table 2 that the crystal sizes of the cobalt oxide-containing catalysts, which are the most active catalysts, are at the highest values. Compared with the active nickel oxide catalysts, it was determined that the nickel oxide-containing catalysts had up to 50% lower average crystal size than the cobalt oxide-containing catalysts. In this case, higher activity was obtained for the CO methanation reaction at large crystal sizes. Although the iron oxide-containing catalysts have high crystal size, they did not show high activity for the CO methanation reaction. This is due to the fact that CO methanation does not prefer the iron oxide active component in the structure. Finally we can conclude that the best performance for CO methanation between the catalysts that contain different metal oxides and prepared with two different preparation methods using different carbon support was obtained from Co_3O_4 graphene oxide supported and traditional impregnation catalyst $\text{Co}_3\text{O}_4/\text{MC_Imp}$ in terms of both CO conversion and CH_4 formation. This catalyst has a lower surface area and a larger average pore diameter compared to other catalysts. Co_3O_4 crystal sizes are larger than catalysts containing NiO. Looking at these results, it can be concluded that the surface area is not very effective for the CO methanation reaction in this study and that the larger average pore diameter and average crystal size are more effective.

Table 4 shows the studies on the methanation reaction using carbon support. When we look at the previous studies in the literature for carbon monoxide methanation, studies with catalysts with similar contents could not be found with the catalysts developed in this study. Therefore, a direct comparison of the results obtained from the activity studies could not be made. Although the results cannot be directly compared, the studies are shown in the table in order to make a comparison. It can be said by looking at Table 4 that the results obtained from our study are much better. If Table 3 and Fig. 12 are compared, it can be seen that cobalt oxide-containing catalysts have better results than the CO methanation catalytic activity results obtained over ruthenium-containing graphitic carbon-supported catalysts given in Table 4. The Co_3O_4 /graphene oxide and Co_3O_4 /activated carbon catalysts, prepared by the impregnation method, gave 100% CO conversion at 225 °C, which is lower than the 100% conversion temperatures given in the literature.

4 Conclusion

In this study, three different carbon supports were used in the structure of the catalysts, which are mesoporous carbon, activated carbon and graphene oxide. And, three different metal oxides were incorporated into the support structure, which are NiO, Co₃O₄ and Fe₂O₃, by using impregnation and co-precipitation techniques. All catalysts were tested for CO methanation reaction. Characteristic and catalytic activity studies proved the effect of the support type, the effect of metal oxide type, and the effect of the preparation method on the characteristic and catalytic properties of the catalysts. According to N₂ physisorption measurements, after active metal loading on the support component, the surface area of the catalyst was lower than the surface area of the support in activated carbon-supported catalysts. Since the porous structure of the support was blocked by the active component, a decrease in the surface area was observed. The decrease in the surface area was less accelerated in the mesoporous carbon and graphene oxide supported catalyst. In this case, it can be said that mesoporous carbon and graphene oxide supported catalysts are more stable at temperature increase compared to activated carbon-supported catalysts. However, activated carbon and mesoporous carbon-supported catalysts gave higher surface area results. The diffraction peaks due to the Carbon, NiO, Co₃O₄ and Fe₂O₃ were detected in XRD measurements according to the catalysts structure. According the average crystal size results, the larger crystals were obtained in cobaltoxide-containing catalysts. The highest activity results for CO methanation were obtained from the catalysts prepared by the impregnation method. Although graphene supported catalysts have lower surface areas than other catalysts, higher activity was obtained in CO methanation. In this case, among the carbon supports studied, the graphene support was determined as the most suitable for CO methanation. Among the active components of NiO, Fe₂O₃ and Co₃O₄, it is known that NiO is the most suitable active component for CO methanation. In this study, catalysts containing Co₃O₄ showed higher activities in CO methanation. Here, it can be said that the interaction of the active component with the support plays an important role. The distribution and size of the active component within the support pores affected the activity results for CO methanation. Higher active component crystal size was obtained in catalysts containing Co₃O₄. In this case, it can be said that CO methanation prefers both the active ingredient Co₃O₄ and larger crystals. The graphene oxide support and Co₃O₄ active component in the catalyst structure provided higher catalytic activity. Co₃O₄/graphene oxide catalyst prepared by the impregnation method leads to 100% CO conversion, 85% CH₄ formation at 275 °C.

Acknowledgements As the project team, we would like to thank Gazi University Scientific Research Unit for their financial support with the project numbered 18/2017-01.

References

- Zeng, Q.; Li, Z.; Zhou, Y.: Synthesis and applications of carbon nanotubes. *J. Nat. Gas Chem.* **15**, 235–246 (2006)
- Yang, Y.; Chiang, K.; Burke, N.: Porous carbon-supported catalysts for energy and environmental applications: A short review. *Catal. Today* **178**, 197–205 (2011)
- Sanchez, E.; Yang, Y.; Find, J.; Braun, Th.; Schoonmaker, R.; Belz, T.; Sauer, H.; Spillecke, O.; Uchida, Y.; Schlögl, R.: Element carbon as catalytic material: Recent trends and perspectives. *Sci. Technol. Catal.* **212**, 317–326 (1999)
- Chen, L.; Song, G.; Fu, Y.; Shen, J.: The effects of promoters of K and Zr on the mesoporous carbon supported cobalt catalysts for Fischer–Tropsch synthesis. *J. Coll. Interf. Sci.* **368**, 456–461 (2011)
- Díaz, J.A.; Fernández, M.M.; Romero, A.; Valverde, J.L.: Synthesis of carbon nanofibers supported cobalt catalysts for Fischer–Tropsch process. *Fuel* **111**, 422–429 (2013)
- Díaz, J.A.; Osa, A.R.; Sánchez, P.; Romero, A.; Valverde, J.L.: Influence of CO₂ co-feeding on Fischer–Tropsch fuels production over carbon nanofibers supported cobalt catalyst. *Catal. Commun.* **44**, 57–61 (2013)
- Díaz, J.A.; Akhavan, H.; Romero, A.; García-Minguillan, A.; Romero, R.; Giroir-Fendler, A.; Valverde, J.L.: Cobalt and iron supported on carbon nanofibers as catalysts for Fischer–Tropsch synthesis. *Fuel Proces. Technol.* **128**, 417–424 (2014)
- Díaz, J.A.; Romero, A.; García-Minguillan, A.M.; Giroir-Fendler, A.; Valverde, J.L.: Carbon nanofibers and nanospheres-supported bimetallic (Co and Fe) catalysts for the Fischer–Tropsch synthesis. *Fuel Proces. Technol.* **138**, 455–462 (2015)
- Ubago-Perez, R.; Carrasco-Marin, F.; Moreno-Castilla, C.: Carbon-supported Pt as catalysts for low-temperature methanol decomposition to carbon monoxide and hydrogen. *Appl. Catal. A Gen.* **275**, 119–126 (2004)
- Xuezi, D.; Jinghong, Z.; Gang, Q.; Ping, L.; Xinggui, Z.; De, C.: Carbon nanofiber-supported Ru catalysts for hydrogen evolution by ammonia decomposition. *Chin. J. Catal.* **31**, 979–986 (2010)
- Donphaia, W.; Faungnawakij, K.; Chareonpanicha, M.; Limtrakul, J.: Effect of Ni-CNTs/mesocellular silica composite catalysts on carbon dioxide reforming of methane. *Appl. Catal. A Gen.* **475**, 16–26 (2014)
- Palacioa, R.; Gallego, J.; Gabelica, Z.; Batiot-Dupeyrat, C.; Barrault, J.; Valangea, S.: Decomposition of ethanol into H₂-rich gas and carbon nanotubes over Ni, Co and Fe supported on SBA-15 and Aerosil. *Appl. Catal. A Gen.* **504**, 642–653 (2015)
- Chiou, J.Y.Z.; Kung, H.Y.; Wang, C.B.: Highly stable and active Ni-doped ordered mesoporous carbon catalyst on the steam reforming of ethanol application. *J. Saudi Chem. Soci.* **21**(2), 205–209 (2017)
- Meng, T.; Xu, Q.Q.; Li, Y.T.; Chang, J.L.; Ren, T.Z.; Yuan, Z.Y.: Nickel nanoparticles highly dispersed on reduced graphene oxide for ammonia decomposition to hydrogen. *J. Ind. Eng. Chem.* **32**, 373–379 (2015)
- Surisetty, V.R.; Tavasoli, A.; Dalai, A.K.: Synthesis of higher alcohols from syngas over alkali promoted MoS₂ catalysts supported on multi-walled carbon nanotubes. *Appl. Catal. A Gen.* **365**, 243–251 (2009)



16. Kim, T.W.; Kim, M.J.; Chae, H.J.; Ha, K.S.; Kim, C.U.: Ordered mesoporous carbon supported uniform rhodium nanoparticles as catalysts for higher alcohol synthesis from syngas. *Fuel* **160**, 393–403 (2015)
17. Jiménez, V.; Sánchez, P.; Panagiotopoulou, P.; Valverde, J.L.; Romero, A.: Methanation of CO, CO₂ and selective methanation of CO, in mixtures of CO and CO₂, over ruthenium carbon nanofibers catalysts. *Appl. Catal. A Gen.* **390**, 35–44 (2010)
18. Li, B.; Wang, C.; Yi, G.; Lin, H.; Yuan, Y.: Enhanced performance of Ru nanoparticles confined in carbon nanotubes for CO preferential oxidation in a H₂-rich stream. *Catal. Today*. **164**, 74–79 (2011)
19. Niu, T.; Liu, G.L.; Liu, Y.: Preparation of Ru/graphene-mesoporous SiO₂ composite and their application to the preferential oxidation of CO in H₂-rich gases. *Appl. Catal. B Environ.* **154–155**, 82–92 (2014)
20. Chen, J.; Cao, F.; Qu, R.; Gao, X.; Cen, K.: Bimetallic cerium—copper nanoparticles embedded in ordered mesoporous carbons as effective catalysts for the selective catalytic reduction of NO with NH₃. *J. Coll. Interf. Sci.* **456**, 66–75 (2015)
21. Romero-Sáez, M.; Dongil, A.B.; Bentino, N.; Espinoza-González, R.; Escalona, N.; Gracia, F.: CO₂ methanation over nickel-ZrO₂ catalyst supported on carbon nanotubes: A comparison between two impregnation strategies. *Appl. Catal. B Environ.* **237**, 817–825 (2018)
22. Wang, W.; Chu, W.; Wang, N.; Yang, W.; Jiang, C.: Mesoporous nickel catalyst supported on multi-walled carbon nanotubes for carbon dioxide methanation. *Int. J. Hyd. Energy* **41**, 967–975 (2016)
23. Dey, S.; Dhal, G.C.: Cerium catalysts applications in carbon monoxide oxidations. *Mater. Sci. Energy Technol.* **3**(6), 24 (2020)
24. Romero-Sáez, M.; Dongil, A.B.; Benito, N.; Espinoza-González, R.; Escalona, N.; Gracia, F.: CO₂ methanation over nickel-ZrO₂ catalyst supported on carbon nanotubes: A comparison between two impregnation strategies. *Appl. Catal. B Environ.* **237**, 817–825 (2018)
25. Truszkiewicz, E.; Kowalczyk, K.; Debska, A.; Wojda, D.; Iwanek, E.; Kepinski, L.; Mierzwa, B.: Methanation of CO on Ru/graphitized-carbon catalysts: Effects of the preparation method and the carbon support structure. *Int. J. Hyd. Energy* **45**, 31985–31999 (2020)
26. Gödde, J.; Merko, M.; Xia, W.; Muhler, M.: Nickel nanoparticles supported on nitrogen-doped carbon nanotubes are a highly active, selective and stable CO₂ methanation catalyst. *J. Energy Chem.* **54**, 323–331 (2021)
27. Ahmad, K.N.; Isahak, W.N.R.W.; Rosli, M.I.; Yusop, M.R.; Kassim, M.B.; Yarmo, M.A.: Rare earth metal doped nickel catalysts supported on exfoliated graphitic carbon nitride for highly selective CO and CO₂ methanation. *Appl. Surf. Sci.* **571**, 151321 (2022)
28. Xiong, J.; Dong, X.; Li, L.: CO selective methanation in hydrogen-rich gas mixtures over carbon nanotube supported Ru-based catalysts. *J. Nat. Gas. Chem.* **21**, 445–451 (2012)
29. Lawal, I.A.; Lawal, M.M.; Azeez, M.A.; Ndungu, P.: Theoretical and experimental adsorption studies of phenol and crystal violet dye on carbon nanotube functionalized with deep eutectic solvent. *J. Mol. Liquids* **288**, 110895 (2019)
30. Cui, G.Y.; Wang, C.Y.; Xiang, G.Q.; Zhou, B.: An electrochemical sensor based on nitrogen doped carbon material prepared from nitrogen-containing precursors. In: IOP Conference Series: Materials Science Engineering. **292**, 012034 (2018)
31. Wibawa, P.J.; Nur, M.; Asy'ari, M.; Nur, H.: SEM, XRD and FTIR analyses of both ultrasonic and heat generated activated carbon black microstructures. *Heliyon* **6**(3), e03546 (2020)
32. Aravind, M.; Amalanathan, M.: Structural, morphological, and optical properties of country egg shell derived activated carbon for dye removal. *Mater. Today Proc.* **43**(2), 1491–1495 (2021)
33. Ramesh, S.; Karuppasamy, K.; Vikraman, D.; Kim, E.; Sanjeeb, L.; Lee, Y.J.; Kim, H.S.; Kim, J.H.; Kim, H.S.: Hierarchical Co₃O₄ decorated nitrogen-doped graphene oxide nanosheets for energy storage and gas sensing applications. *J. Ind. Eng. Chem.* **101**, 253–261 (2021)
34. Hussain, I.; Jalil, A.A.; Hassan, N.S.; Farooq, M.; Mujtaba, M.A.; Hamid, M.Y.S.; Sharif, H.M.A.; Nabgan, W.; Aziz, M.A.H.; Owgi, A.H.K.: Contemporary thrust and emerging prospects of catalytic systems for substitute natural gas production by CO methanation. *Fuel* **311**, 122604 (2022)
35. Kang, S.H.; Ryu, J.H.; Kim, J.H.; Seo, S.J.; Yoo, Y.D.; Sai Prasad, P.S.; Lim, H.; Byun, C.D.: Co-methanation of CO and CO₂ on the Ni_x-Fe_{1-x}/Al₂O₃ catalysts; effect of Fe contents. *Korean J. Chem. Eng.* **28**(12), 2282–2286 (2011)
36. Derekaya, F.; Arasan, N.; Güldür, Ç.: Development of NiFeSi mixed oxide catalysts For CO methanation. *Chem. Pap.* **76**, 841–854 (2022)
37. Jiménez, V.; Sánchez, P.; Panagiotopoulou, P.; Valverde, J.L.; Romero, A.: Methanation of CO, CO₂ and selective methanation of CO, in mixtures of CO and CO₂, over ruthenium carbon nanofibers catalysts. *Appl. Catal. A Gen.* **390**, 35–44 (2010)
38. Variava, M.F.; Church, T.L.; Noorbehesht, N.; Harris, A.T.; Minett, A.I.: Carbon-supported gas-cleaning catalysts enable syn gas methanation at atmospheric pressure. *Catal. Sci. Technol.* **5**, 515 (2015)
39. Gonçalves, L.P.L.; Sousa, J.P.S.; Salomé, O.; Soares, G.P.; Bondarchuk, O.; Lebedev, O.I.; Kolen'ko, Y.V.; Pereira, M.F.R.: The role of surface properties in CO₂ methanation over carbon-supported Ni catalysts and their promotion by Fe. *Catal. Sci. Technol.* **10**, 7217 (2020)

Springer Nature or its licensor (e.g. a society or other partner) holds exclusive rights to this article under a publishing agreement with the author(s) or other rightsholder(s); author self-archiving of the accepted manuscript version of this article is solely governed by the terms of such publishing agreement and applicable law.